Improvements in a Calorimeter for High-Power CW Lasers

GEORGE E. CHAMBERLAIN, PHILIP A. SIMPSON AND RICHARD L. SMITH

Abstract—**Measurement certainty with the BB series of electrically calibrated calorimeters for high-energy lasers has been enhanced by the addition of monitors for energy backscattered from the meter and for energy missing the entrance aperture (overspill). The performance and design features of the recently constructed BB2 meter are compared with the previously described BB1 meter. Direct intercomparison shows the agreement between meters to be 1 percent.**

I. Introduction

A PREVIOUS article, Smith *et al.* [1], describes a calorimeter constructed by NBS for measuring the energy of high-power CW laser beams. The calorimeter has been designated BB1. Since 1973, BB1 has been used as a reference meter for intercomparisons with other non-NBS high-energy laser (HEL) calorimeters.

We describe here improvements in BB1 and design changes incorporated in a similar calorimeter, BB2, that have been implemented as a result of our experience with BB1. Smith [1] covers the optical and thermal design, theory of the measurement process, electrical and backscatter calibration procedures, and imprecision and inaccuracy estimates for BB1. We do not repeat those discussions here except as needed for clarity.

A significant error in laser radiation measurements is frequently made if energy is not accounted for when a portion of the incident radiation is backscattered out of the receiver unit and/or does not enter the receiver. Section II describes a method we have used to monitor energy backscattered out of the BB calorimeters. Section III describes an overspill monitor used to detect radiation that impinges on the calorimeter outside of the entrance aperture. To our knowledge, this is the first time that quantitative measurements of backscatter and overspill have been made on a run-to-run basis for laser power and energy measurements. The principles espoused here are not limited to HEL measurements, and their adoption will increase the integrity of laser beam parameter measurements in general.

Section IV describes design changes incorporated in the BB2 calorimeter and compares the response of BB2 to the response of BB1 for high-energy laser injection.

Section V gives a characterization of the BB2 calorimeter based on electrical calibrations and the results of intercomparing BB2 with BB1.

Manuscript received September 26, 1977.
The authors are with the National Bureau of Standards, Boulder, CO. 80302.

II. Backscatter Monitor

The purpose of a backscatter monitor is to provide assurance on a run-to-run basis that the calorimeter backscatter is within acceptable limits. Any geometric or optical change in the surfaces of the calorimeter would likely cause a change in the backscatter. The BB calorimeters are field instruments and as such they undergo severe physical jolting in being transported, which might cause a change in the cavity geometry. In addition, the combination of exposure to wind, dust, moisture, and high levels of laser beam flux could lead to changes in the optical properties of the cavity surfaces.

Fig. 1 illustrates how the backscatter monitor (BSM), and the overspill monitor (OSM) discussed in Section III, are used. The BSM consists of an aperture plate placed in front of the four-sided horn leading to the optical cavity. This plate intercepts a portion (about 10 percent) of the radiation coming back out of the horn. The excess radiation that goes out through the aperture is lost as backscatter. Radiation from the cavity that is absorbed by the backscatter monitor remains within the calorimeter and is not a component of backscatter. The hard anodized surface of the aluminum plate has an absorption coefficient greater than 95 percent for the CO_2 radiation band (9–11 μm) at which the BB calorimeters have been used. Thermal sensors mounted on the plate provide analog output signals.

The backscatter monitor plate for BB1 differs somewhat from the BB2 BSM plate which is shown in Fig. 1. The

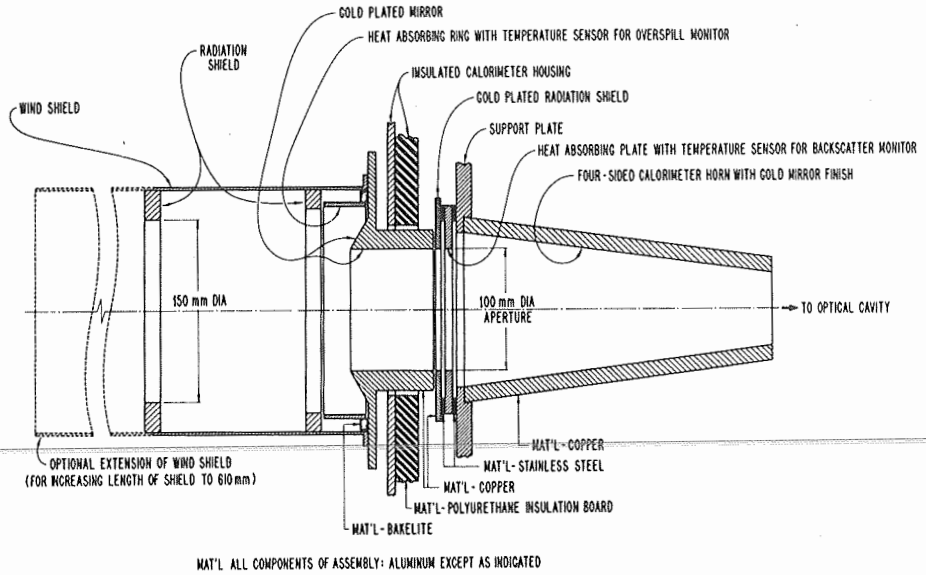

Fig. 1. Cross sectional views of the backscatter monitor used on the BB2 calorimeter, and the overspill monitor used on the BB1 and BB2 calorimeters.

BB1 plate is 203 mm square by 4.8 mm thick. The 10-cm diameter aperture in the plate defines the entrance aperture of the calorimeter. A 25-mm wide annular region around the aperture is thinned down on the side facing the horn to 1.3 mm thick to enhance the sensitivity. 1.6-mm wide by 1.0-mm deep channels are cut into the front side to hold thermocouples. Six "hot" junctions are located around the entrance aperture and 6.4 mm from the edge; the six "cold" junctions located near the outer edge of the plate are well removed from view of the 127-mm square horn. A 25-mm wide gold-plated brass ring covers the BSM plate around the entrance aperture and serves as a radiation shield. The plate is mounted near its edges directly to an aluminum frame and without the stainless-steel spacer shown for BB2.

The geometry of the BB2 BSM plate, see Fig. 1, is simpler than that for BB1 and consists of a flat plate which is 6.4 mm thick and 171 mm square and has a 10-cm diameter aperture. Resistive temperature sensors are used to average the temperature over a larger area than for BB1 and because they have a larger temperature sensitivity than thermocouples. Two 10-mm wide by 102-mm long sensors are positioned with one on each side of the plate next to the mounting spacer and in the shadow of the horn. Two reference sensors are mounted on the plate supporting the horn and BSM assembly. The BSM plate makes thermal contact with the support plate through a 3.2-mm thick stainless-steel spacer located around the periphery. A radiation shield is mounted in front of the BSM plate with a second stainless steel spacer.

Fig. 2(a) shows the response of the BB1 backscatter monitor to high-energy laser radiation of short duration. The BB1 monitor was designed for high sensitivity and has a multimodal response. The decay portion of the output signal is not fully described by even a two-time constant exponential model [2]. The time constant for the strong fast component(s) is less than 3 s, and for the slow component(s) it exceeds 40 s. In most cases, the BB1 monitor

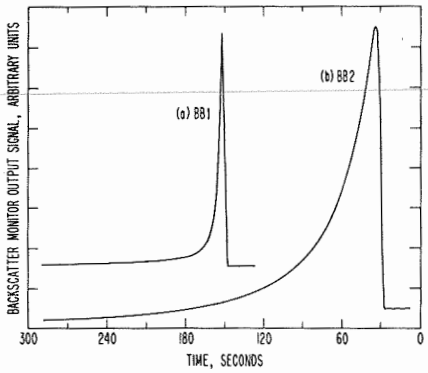

Fig. 2. Response of the BB backscatter monitors to high-power laser radiation.

output peaks in less than one second after beam turnoff.

The baseline-to-peak excursion is taken as the reading for the BB1 backscatter monitor. Calibration of the monitor was obtained by inputting a low-power, 200–500 W, CO_2 laser beam to the calorimeter, measuring the energy backscattered [1], and noting the monitor reading. Beam injection times of 2 to 120 s were used to determine the calibration curve as a function of injection time.

Calibrations were made for input beam positions along the vertical center-line of the 10-cm aperture for a distance of 3.5 cm above and below the center. Over this measurement range the backscatter fraction varies from 0.2 to 2.4 percent. The complex structure of the horn and cavity is most certainly the source of large variations of backscatter fraction with position. Within the scatter of the data the backscatter monitor calibration is independent of the input beam position.

Apparent backscatter is the amount of backscattered energy estimated from the monitor reading using the calibration factor. The apparent backscatter of BB1 for high-energy large-area laser beams varies from 1 to 2 percent. This range of apparent backscatter agrees well with the assigned value of 1 percent and is within the stated range of uncertainty of 0 to 2.3 percent.

The BB2 backscatter monitor was designed for suppression of high-order modes in its response, simplicity, and ruggedness. After reaching a peak value, the monitor response, see Fig. 2(b), is fully described by two decaying exponentials. The time constants are 20 and 63 s. At beam turnoff the output is about ⅓ to ½ of the peak value, and the peak occurs about 4 s later. A measure of the small amplitude of the faster modes is the approximately 5 percent difference in area under the curve in Fig. 2(b) compared to that for the two-time constant model which is fitted to the response. The shift in the baseline level is due to the temperature offset that occurs between the monitor plate and the reference plate as the calorimeter warms up. The baseline shift is less than 10 percent of the peak signal rise and is of minor consequence in characterizing the monitor.

Preliminary calibration of the BB2 backscatter fraction and the backscatter monitor response have been made with a scan procedure similar to that for BB1. The backscatter fraction varies from 0.04 to 2.4 percent along the vertical centerline of the aperture. The average of observed values of 1 percent is assigned as the nominal backscatter.

Another difficulty with the BB2 monitor is the factor of 30 loss in peak signal to noise compared to the BB1 monitor. Direct calibration of the peak response cannot be made for short injection times because of inadequate laser power. Ninety second injections from a 200-W laser were used for the initial calibration work. With hindsight, and the realization that only 10 percent of the energy backscattered from the horn is intercepted by the monitor, one can use a thinner plate to gain back some of the lost sensitivity.

A two-time constant model [2] has been used to relate the BB2 monitor response curve for calibration beams of low-power to that for high-power beams. The apparent backscatter fractions for high power inputs are considerably less than 1 percent. These low values are unexpected and based on meager data. Further measurements are necessary to verify their reality.

The larger values of the apparent backscatter fraction (>1.5 percent) for BB1 were correlated with significant overspill (>1 percent) at the entrance aperture. The correlation suggests that, for beam inputs near the periphery of the entrance aperture, either the backscatter fraction increases or the monitor calibration is changed due to a change in the distribution of the backscattered energy. For BB2, the preliminary calibrations indicate that the monitor calibration is not independent of the position of the input beam along the vertical center line of the entrance aperture.

It is apparent that in order to utilize the BSM to reduce the error budget for backscatter of the BB calorimeters it is necessary to calibrate the backscatter monitors for positions of the input beam over a much larger region of the entrance aperture than has been done.

III. Overspill Monitor

The purpose of an OSM on the BB calorimeters is to flag a laser run when too large of a fraction of the beam is not measured due to missing the entrance aperture. Losses as large as 50 percent have been encountered in the field. Frequently crude overspill monitors are used such as masking tape or plexiglass apertures. The lack of a quantitative measure of overspill led us to design an overspill monitor. Used as a calorimeter, the OSM can measure the overspill within a 15-cm aperture with an estimated uncertainty of ±10 percent.

The design of the overspill monitor is shown in Fig. 1. A conical mirror of gold-plated copper directs the overspilled radiation onto an absorbing ring of hard anodized aluminum. Resistive heat sensors are affixed to the outside of the ring. Also attached to the outside of the ring are electrical heaters which enable the response of the ring to be calibrated electrically.

The OSM was tested for varying electrical and 10.6-μm laser beam inputs up to 10 kJ. The agreement between the electrical calibration value and the calibrated laser beam was better than the ±7-percent inaccuracy assignment for the OSM. Adding the imprecision of ±3 percent assigned to the OSM monitor to the inaccuracy yields the estimated ±10-percent limit for the total uncertainty for a single measurement.

IV. BB2 Calorimeter

The performance of the BB2 calorimeter was improved over that of the BB1 calorimeter by making some design changes in its construction, and changes in the length of the rating and settling periods. The BB2 calorimeter is shown in Fig. 3. Some of the thermal properties and operating parameters are given in Table I and compared to the corresponding results for BB1.

The optical cavity geometry remains the same as for BB1; however, the cavity plates for BB2 are individually supported in a rugged frame made from tubular stainless steel. The purpose of the frame is to insure that there is no change in the cavity geometry during transportation. Water circulates through the tubular frame to provide thermal coupling.

For reasons of economy and replaceability without loss of performance, a commercial platinum resistance thermometer and output linearizing electronics are used for the temperature sensor in BB2.

The water pump on BB2 is a compact, efficient, and inexpensive rotary-vane pump which is manufactured for the food processing industry. The internal carbon-graphite structure is suited to pumping water which has a low lubricity. The compact brass housing provides good thermal coupling to the calorimeter. The pump for BB1 is a centrifugal pump with a cast iron housing that is more massive than the BB2 pump. For both calorimeters, the pump is connected to an external motor by a stainless-steel shaft. The parameters in Table I reflect the fact that the BB1 pump has been slowed down to reduce the power of self-heating. At the original speed of 3600 r/min used in [1], the circulation rate was 0.6 l/s and the power input 580 W.

The very quiet operation of the BB2 pump and motor contributes to improved operator performance in the field.

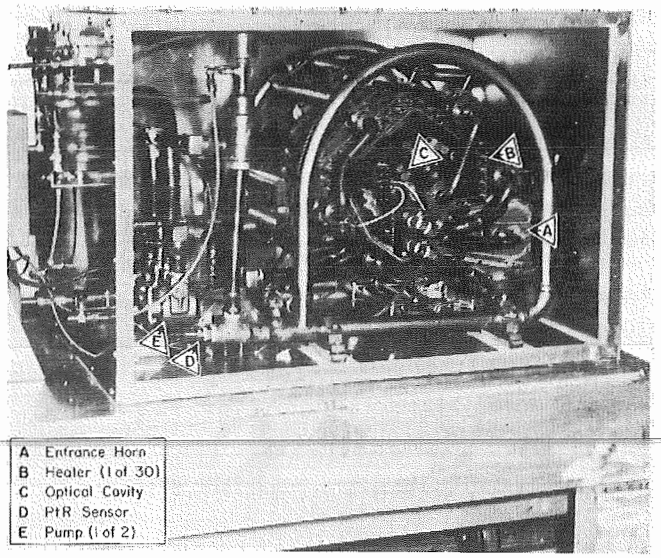

Fig. 3. BB2 calorimeter with side panel removed. (Photo courtesy of the NASA-Lewis Research Center.)

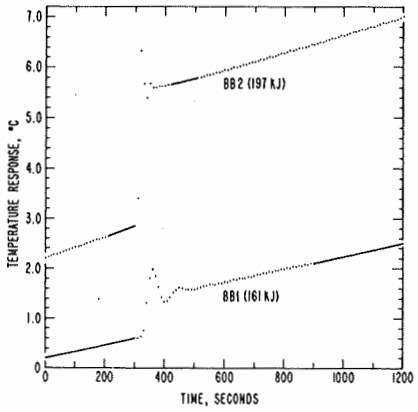

Fig. 4. Response of the BB1 and BB2 calorimeters to high-power laser radiation input. For both curves the output voltage has been converted to the approximate sensor temperature and an arbitrary baseline subtracted. The data are digitized every 10 s. The solid lines show the rating periods used in a least squares fit to determine the response parameters. The duration of laser beam input was less than 10 s.

TABLE I
Comparison of Thermal Properties and Operating Parameters of the BB1 and BB2 Calorimeters

ITEM	BB1	BB2	UNITS
Design power limit	100	100	kW
Design energy limit	6	2.5	MJ
Heat capacity	180	80	kJ/°C
Volume of water	26	7	ℓ
Water circulation rate	.4	.5	ℓ/s
Water circulation time	65	14	s
Power input to calorimeter due to circulating water	180	170	W
Coefficient for heat flow out of calorimeter (h)[a]	3	4	W/°C
Efficiency of stirring[b]	37	52	%
Pump speed	2600	1750	rpm
Rating periods	5	1.5	min
Main, or settling, period	10	2	min

(a) See reference [1].

(b) Ratio of hydraulic power developed to total power input.

Ease of communication with others is permitted and stress due to high noise levels is removed.

The 20-l holding tank designed into BB1 has been omitted from BB2. The four times reduction in round trip time due to the reduced water volume causes the temperature oscillations after heat injection to damp out much faster for BB2 than for BB1. The rapid decay of oscillations is seen in Fig. 4, which compares the responses of the temperature sensors to laser beam injection for the BB1 and BB2 calorimeters.

Reference [1] refers to the procedure for deriving an effective temperature rise of the calorimeter from a four-parameter nonlinear least squares fit to the temperature data. The curve fit is made to two rating periods. The prerating period occurs before energy injection, the post-rating period after energy injection. Ideally, the rating periods are taken for the lowest mode or single time constant exponential response of the calorimeter. The lowest mode time constants of 50 ks and 13 ks for BB1 and BB2, respectively, are so large that a single exponential response is evidenced by an essentially constant rate of change of temperature over a 5-min period.

In the BB2 response curve in Fig. 4, one sees that there is a second mode of about 3.3 min and that it takes about 8 min for the temperature response to settle down to a single exponential dependence on time. A similar second mode for BB1 is partially masked by the slower decay of oscillation, and appears to be of smaller amplitude. We attribute the second mode in both cases to the process of setting up a heat flow gradient from the internal plumbing of the calorimeter to the massive supporting structure.

The rating periods are shown as solid lines in Fig. 4. The main period is the time between rating periods and is the sum of the injection time plus a fixed time for the settling period. Values are given in Table I. For BB2, the rating and settling times have been made as short as practicable to reduce the effect of environmental fluctuations and the amount of self-heating. The minimum run time of 20 min for BB1 is reduced to 5 min for BB2.

An approximate estimate of the effect of environmental temperature fluctuation is in agreement with our experience with BB1. Suppose there is an effective noise of 1°C in the environmental temperature fluctuations. Then, with a 4 W/°C heat flow coefficient (Table I), and a 20-min run time, the noise, or uncertainty, in heat lost from the calorimeter is (4 W/°C) × 1°C × 1200 s or 5 kJ. For a nominal 60-kJ run the 5-kJ uncertainty is 8 percent. We have seen deviations in the electrical calibration factor up to 4 percent under adverse weather conditions.

The effect on BB2 of changing the settling period from 10 min to 2 min is to change the corrected temperature rise by about 6 percent. This change occurs because the higher mode in the response curve is now included in the post-rating period. This change in corrected rise is about the same for either laser or electrical heat input. Therefore, the

1-percent allowance in the BB1 error budget for bias due to inequivalence in the response to electrical and laser energy inputs remains valid for the BB2 calorimeter.

Another possible source of unknown heat loss is wind blowing directly into the entrance aperture of the calorimeter. A windshield was made which is a tube that extends the shield of the overspill monitor to a length of three diameters. The windshield has not yet been used in field measurements. A potential drawback to the windshield is that the creation of a static air mass can cause thermal blooming. However, the occurrence of blooming would be detected by the overspill monitor.

V. Characterization and Comparison of BB2 and BB1 Calorimeters

The electric substitution method is used to determine the calibration factor for the BB calorimeters. Characterization of the BB2 calorimeter based on electrical calibrations is given in Table II. The BB1 characterization is included for comparison. Figs. 5 and 6 are control charts for the BB2 electrical calibration factors versus row, or sequence number, and versus input energy.

For each electrical calibration run, a calibration factor is determined which is the ratio of the effective temperature rise to the input energy. The temperature is expressed as the equivalent volts of output of the temperature sensor. By definition, N is the number of electrical calibrations, K_{el} is the average of, and s is the standard deviation of the electrical calibration factors. The calibration factor K used for laser energy input may differ from K_{el} owing to systematic effects in the calorimeter and/or electrical calibration system. The 1-percent factor given in row 4 of Table II accounts for the nominal 1-percent backscatter of the calorimeters.

The inaccuracy given in row 5 is composed of the sum of estimated systematic errors and this imprecision in the mean for K_{el}. The imprecision in the mean is calculated as $\pm t \times s \times N^{-1/2}$ where t is the statistic used for calculating the confidence interval of the mean. The imprecision is ±0.2 percent for both calorimeters. A two-sided 95-percent confidence interval has been used. The budget of systematic errors for both calorimeters is (cf. [1]): ±0.3 percent for electrical energy, ±1.3 percent for backscatter, and ±1.0 percent for the inequivalence in calorimeter response between laser and electrical energy inputs. Cases in which overspill monitor readings are used to correct energy readings are the exception and adjustments in the error budget are necessary (cf. Section III).

The imprecision for a single measurement of laser energy (row 6, Table II) is calculated as $\pm 1.96 \times A \times s$. The A statistic is tabulated by Natrella [3] and is the factor used to estimate a one-sided upper bound for the standard deviation. The A statistic can be obtained from the χ^2 statistic using the relation

$$A(1 - \alpha,\nu) = [\nu/\chi^2(\alpha,\nu)]^{1/2}.$$

We have used a 95-percent confidence level ($\alpha = 0.05$) for the A statistic. The degrees of freedom ν are $N - 1$.

TABLE II
Characterization of BB1 and BB2 Calorimeters for 10.6-μm Radiation

ROW	ITEM	BB1	BB2	UNITS
1.	Number of electrical calibrations (N)	35	13	
2.	Residual standard deviation of electrical calibration (s)	.7	.4	%
3.	Calibration constant for laser energy (K)	2.7	2.4	MJ/V
4.	Correcting factor for systematics (K/K_{el})	1.01	1.01	
5.	Inaccuracy[a]	± 2.8	± 2.8	%
6.	Imprecision[a]	± 1.8	± 1.2	%
7.	Uncertainty[a]	± 4.6	± 4.0	%

[a] Estimated values for a single measurement of laser energy.

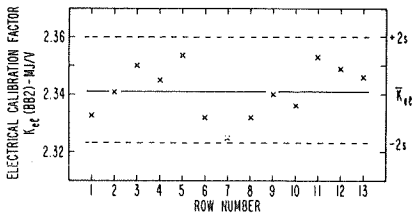

Fig. 5. Control chart of the electrical calibration factor for the BB2 calorimeter versus observations in chronological order.

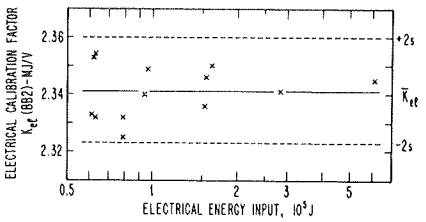

Fig. 6. Control chart of the electrical calibration factor for the BB2 calorimeter versus the input energy.

The total uncertainty given in row 7 of Table II is the sum of rows 5 and 6.

The BB2 calorimeter has been intercompared with BB1 by means of the beam splitter technique [4] and using the 10.6-μm beam for a gas dynamic laser. A rotating, sectored, metal mirror divides the laser beam into a transmitted beam and a reflected beam. Six runs were taken, three with BB2 in the transmitted beam position, and three with BB1 in the transmitted beam position. A linear least squares fit to the logarithm of the ratio of observed energies is used to determine the beam splitter ratio, and the ratio of BB2 readings relative to BB1 readings.

The intercomparison resulted in a residual standard deviation of 0.6 percent, a ratio of readings for BB2 versus BB1 of 0.991, and an imprecision in the mean for the ratio of ±0.7 percent. That is, based on the statistics of the intercomparison alone, the bias between the two calorimeters is at least 0.2 percent and not greater than 1.6 percent at the 95-percent confidence level. The observed difference of 0.9 percent is well within the error budget for either calorimeter and strongly supports the error analysis. One

expects the offset to be less than the systematics in the error budget because the calorimeters are calibrated from a common source; and since their construction is similar, the backscatter and inequivalence should also be similar. The offset in calibration may well be due to small changes in the backscatter and inequivalence.

The 0.6-percent residual standard deviation of the BB2/BB1 intercomparison is the smallest value we have seen in the three year period of approximately ten intercomparisons of HEL meters with the BB1 calorimeter.

VI. Summary

Reference [1] describes the BB1 calorimeter system for measuring the energy content of CW high-energy laser beams to better than 4-percent total uncertainty. In this article, we describe several improvements in the design and operation of a water-stirred calorimeter. In particular, we have implemented the use of a backscatter monitor and overspill monitor to give diagnostic checks on every laser run. A windshield is used to reduce the effect of wind in an open field environment. A second calorimeter BB2 has been put into operation and shown by direct intercomparison to have an offset of less than 1 percent from the BB1 calorimeter. The performance of BB2 has been enhanced by changes incorporated into its design and operation. Plumbing changes have reduced the rate of self-heating and permitted a reduction from 20 min (BB1) to 5 min time per run.

Acknowledgment

The BB calorimeter systems are now being maintained by the Aerospace Guidance and Metrology Center (AGMC) of the Newark AFS, Newark, OH. We wish to thank R. O. Wellington of AGMC for allowing us to use the results of intercomparison of the BB calorimeters and data for the BB2 calibration history. The intercomparison of BB1 and BB2 was conducted at The Sandia Optical Range (SOR) of the Kirtland AFB, Albuquerque, NM. Captain D. Caldwell of the SOR coordinated the intercomparison. We also appreciate the support of funding by NASA and the following DOD groups: The Calibration Coordination Group (CCG), AFWL, MICOM, NRL, ARPA, and AGMC.

References

[1] R. L. Smith, T. W. Russell, W. E. Case, and A. L. Rasmussen, "A calorimeter for high-power CW lasers," *IEEE Trans. Instrum. Meas.*, vol. IM-21, pp. 434–438, Nov. 1972.

[2] E. J. Johnson, Jr., "Evaluating the inequivalence and a computational simplification for the NBS laser energy standards," *Appl. Opt.*, vol. 16, pp. 2315–2321, Aug. 1977.

[3] M. G. Natrella, *Experimental Statistics* (NBS Handbook 91). Washington, DC: Government Printing Office, 1966.

[4] E. D. West, W. E. Case, A. L. Rasmussen, and L. B. Schmidt, *J. Res. Nat. Bur. Stand.*, vol. 76A, pp. 13–26, 1972.